Applied Catalysis B: Environmental 97 (2010) 292–298

Contents lists available at ScienceDirect

Applied Catalysis B: Environmental

journal homepage: www.elsevier.com/locate/apcatb

# Evaluation of operating parameters involved in solar photo-Fenton treatment of wastewater: Interdependence of initial pollutant concentration, temperature and iron concentration

A. Zapata[a], I. Oller[a], L. Rizzo[b], S. Hilgert[c], M.I. Maldonado[a,e], J.A. Sánchez-Pérez[d,e], S. Malato[a,e,*]

[a] Plataforma Solar de Almería (CIEMAT), Carretera Senés, Km 4, 04200, Tabernas (Almería), Spain
[b] Department of Civil Engineering, University of Salerno, via Ponte don Melillo, 84084 Fisciano (SA), Italy
[c] Karlsruhe Institut of Technology (KIT), Institut für Wasser und Gewässerentwicklung. Adenauerring 20b, 76131 Karlsruhe, Germany
[d] Departament of Chemical Engineering, University of Almería, Crta de Sacramento s/n, 04120 Almería, Spain
[e] CIESOL, Joint Centre University of Almeria-CIEMAT, 04120 Almeria, Spain

ARTICLE INFO

*Article history:*
Received 7 February 2010
Received in revised form 13 April 2010
Accepted 17 April 2010
Available online 24 April 2010

*Keywords:*
Advanced oxidation processes
Hydrogen peroxide
Pesticides
Solar photocatalysis

ABSTRACT

A mixture of five commercial pesticides (Vydate®, Metomur®, Couraze®, Ditimur-40® and Scala®) commonly used in intensive agriculture has been selected as an example of highly toxic, non-biodegradable wastewater to be treated by solar Photo-Fenton. The effect of the total concentration of organics as dissolved organic carbon (100–500 mg/L), operating temperature (25–50 °C), dissolved iron concentration and their relationship to different process efficiency parameters (mineralization rate, hydrogen peroxide consumption and treatment time) were evaluated. Experiments were carried out under sunlight in a pilot plant. It consists of four compound parabolic collectors (CPCs) and a total volume of 75 L. From the results of the study it can be concluded that solar plants should be designed for operating at temperatures below 45 °C to avoid significant loss of iron. $H_2O_2$ should be carefully dosed during the photo-Fenton treatment to avoid its continued excess and inefficient use.



## 1. Introduction

One of the most pressing worldwide concerns is the current deterioration of the water supply due to economic and industrial growth. A diversity of recalcitrant contaminants due to human activity, from heavy metals to emerging micropollutants are being identified in water in increasing numbers [1]. In the Mediterranean Basin, polluting pesticides from expanding intensive agriculture are accumulating in the environment, and have been designated as Priority Substances (PSs) in EU legislation [2]. Consequently, research has focused on developing new methods as alternatives to the conventional activated sludge treatment for decontaminating water containing toxic or non-biodegradable organic compounds. In this context, Advanced Oxidation Processes (AOPs) have been described as effective methods for oxidizing these substances due to their capacity for mineralizing almost any organic contaminant [3,4]. Several recent studies have demonstrated the effectiveness of AOPs for decontamination of a wide range of industrial wastewater at laboratory and pilot plant scale [5–7]. Nevertheless, full scale applications are still rare since these novel techniques are not yet cost-competitive [8,9]. As a result, recent investigation has been directed at finding cost-reducing measures for making AOPs economically feasible options for industrial-scale wastewater treatment. One of these measures is the use of renewable energy sources, for instance sunlight as the irradiation source, for running the AOP. This approach makes the new technology not only more cost-effective but also more environmentally friendly. In recent years, concern about the environmental impact of these innovative processes has been raised, and many tools, such as Life Cycle Assessment (LCA), have been applied to evaluate and minimize their impact [10,11]. In this context, optimization of AOPs by targeting their cost and environmental impact is essential for further industrial application of the proposed systems [12]. Among AOPs, photo-Fenton has attracted much attention, not only because of its excellent mineralization of almost any type of organic pollutant, but also because it can be driven by solar irradiation [13]. Real pesticide wastewaters are usually at acid pH because pesticide and plant nutrients as phosphoric and nitric acid are jointly managed, favoring the application of photo-Fenton which is more efficient at acid pH. The main solar photo-Fenton parameters that must be optimized to reduce its cost and its environmental impact as much as possible are $H_2O_2$ consumption and the size (surface area) of the solar collector field necessary to drive the process. This study therefore focuses on the evaluation of some impor-

* Corresponding author. Tel.: +34 950 387940; fax: +34 950 365015.
*E-mail address:* sixto.malato@psa.es (S. Malato).

0926-3373/$ – see front matter © 2010 Elsevier B.V. All rights reserved.
doi:10.1016/j.apcatb.2010.04.020

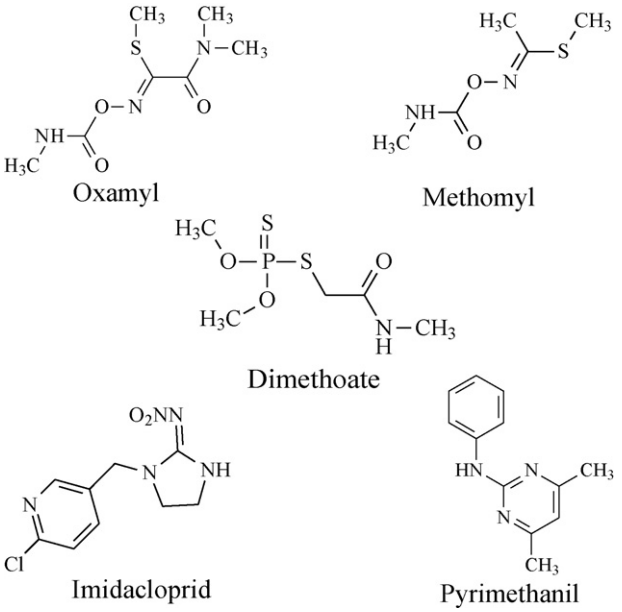


**Diagram 1.** Pesticide chemical structures.

tant operating parameters affecting the kinetics (higher kinetics leads to a smaller solar collector field) of the solar photo-Fenton treatment of water containing pesticides in order to find the best operating conditions (the lowest $H_2O_2$ consumption). The results would be more useful if extrapolated to a real situation containing mixtures of different contaminants. Therefore, a mixture of five commercial pesticides commonly used in intensive agriculture has been selected as an example of highly toxic, non-biodegradable wastewater which must be treated by innovative decontamination technologies such as photo-Fenton. The effect of the total concentration of organics as dissolved organic carbon (DOC) (Vydate®, Metomur®, Couraze®, Ditimur-40® and Scala®), operating temperature, dissolved iron concentration and their relationship to different process efficiency parameters (mineralization rate, hydrogen peroxide consumption and treatment time) were evaluated. It is well known that these parameters affect the overall kinetics, and consequently they have been thoroughly studied by several authors, as reviewed recently by Pignatello et al. [14], but not as a whole (interdependencies between different variables and parameters) and taking into account treatment plant design and operation. The objective of obtaining an integrated design of solar plants specific operational parameters, as it has been intended in this paper, has not yet investigated. Our final goal is to better understand the process as a whole in order to design a future scaled-up photo-Fenton system for treating industrial wastewater containing different contaminants at high concentrations (hundreds of mg/L).

## 2. Experimental

### 2.1. Chemicals

Commercial formulations of Vydate® (10%, w/v oxamyl, $C_7H_{13}N_3O_3S$), Metomur®, (20%, w/v methomyl, $C_5H_{10}N_2O_2S$), Couraze® (20%, w/v imidacloprid, $C_{16}H_{22}ClN_3O$), Ditimur-40® (40%, w/v dimethoate, $C_5H_{12}NO_3PS_2$) and Scala® (40%, w/v pyrimethanil, $C_{12}H_{13}N_3$) were used as received. Diagram 1 shows their chemical structures. Analytical standards (>98%) for chromatographic analyses were purchased from Sigma–Aldrich.

Distilled water used in the pilot plant was supplied by the Plataforma Solar de Almería (PSA) distillation plant (conductivity < 10 μS/cm, $Cl^-$ = 0.2–0.3 mg/L, $NO_3^-$ < 0.2 mg/L, organic carbon <0.5 mg/L). The photo-Fenton experiments were performed using $FeSO_4{\cdot}7H_2O$, reagent-grade hydrogen peroxide (30%, w/v) and sulfuric acid for pH adjustment (around 2.7–2.9) all purchased from Panreac.

### 2.2. Analytical determinations

High-performance liquid chromatography (HPLC, Agilent Technologies, series 1100) with a UV-DAD detector and a C-18 column (LUNA 5 μm, 3 mm × 150 mm from Phenomenex) as the stationary phase was used to monitor the pesticide concentrations during degradation. The mobile phase consisted of a mixture of 15% HPLC-grade acetonitrile, and 85% ultrapure water (Millipore Co.). Detection was done at three different wavelengths depending on the active ingredient of the commercial pesticide: 210 nm (dimethoate and pyrimethanil), 234 nm (methomyl and oxamyl) and 270 nm (imidacloprid). Mineralization was followed by measuring the dissolved organic carbon (DOC) by direct injection of filtered samples into a Shimadzu-5050A TOC analyzer with an NDIR detector and calibrated with standard solutions of potassium phthalate. Total iron concentration was monitored by colorimetric determination with 1,10-phenanthroline, according to ISO 6332, using a Unicam-2 spectrophotometer. Hydrogen peroxide was analyzed by a spectrophotometric method using ammonium metavanadate, which allows the $H_2O_2$ concentration to be determined immediately based on a red-orange peroxovanadium cation formed during the reaction of $H_2O_2$ with metavanadate, maximum absorption of which is at 450 nm. The peroxide concentrations are calculated from absorption measurements by a ratio found by Nogueira et al. [15].

### 2.3. Experimental set-up

Photo-Fenton experiments were carried out under sunlight in a pilot plant specifically developed for photo-Fenton applications, installed at the Plataforma Solar de Almeria (PSA). It is equipped with on-line measurement sensors for T, pH and dissolved oxygen, and connected to a PC for remote data acquisition and process control decisions. The plant also incorporates heating and cooling devices to control reaction solution temperatures during experiments. A diagram of this system has been published elsewhere [16]. It consists of four compound parabolic collectors (CPCs), a reservoir tank, a recirculation pump and connecting tubing. Solar ultraviolet radiation (UV) was measured by a global UV radiometer (KIPP&ZONEN, model CUV 3) mounted on a platform tilted 37° (the same as the CPCs). With Eq. (1), combination of the data from several days' experiments and their comparison with other photocatalytic experiments is possible [17].

$$t_{30W,n} = t_{30W,n-1} + \Delta t_n \frac{UV}{30}\frac{V_i}{V_T}; \quad \Delta t_n = t_n - t_{n-1} \tag{1}$$

where $t_n$ is the experimental time for each sample, UV is the average solar ultraviolet radiation measured during $\Delta t_n$, and $t_{30W}$ is a "normalized illumination time". In this case, time refers to a constant solar UV power of 30 W/m (typical solar UV power on a perfectly sunny day around noon). $V_T$ is the total volume of the water loaded in the pilot plant (75 L), $V_i$ is the total irradiated volume (44.6 L).

All photo-Fenton experiments were carried out at a pH adjusted to 2.7–2.9 and hydrogen peroxide concentration kept between 100 and 300 mg/L throughout the process. The mixture of pesticides was added directly into the pilot plant and homogenized by turbulent recirculation for half an hour. With the collectors covered, the pH was adjusted and iron salt (Fe = 20 mg/L) was added. Then an initial amount of hydrogen peroxide was added (300 mg/L), the collectors were uncovered and photo-Fenton began. Hydrogen peroxide was measured frequently and consumed reagent was

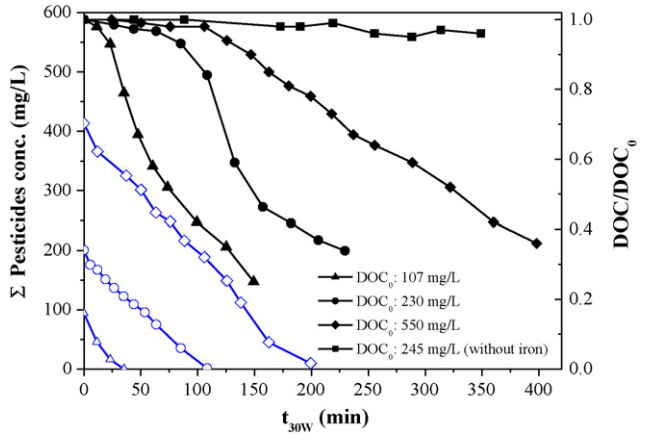


**Fig. 1.** Mineralization (solid symbols) and degradation (open symbols) of the pesticide mixture (20 mg/L $Fe^{2+}$) at different initial DOC concentrations during the photo-Fenton experiments. Blank experiment DOC results (without iron) are also shown.

continuously replaced so as to maintain an excess of $H_2O_2$. Experiments in absence of irradiation were performed in 3-L vessels with continuous agitation under the same conditions as photo-Fenton.

## 3. Results and discussion

The aim of this study is the detailed evaluation of the effect of some of the operating parameters involved in the solar photo-Fenton degradation of wastewater containing a mixture of commercial pesticides (original wastewater organic load, wastewater temperature and dissolved iron concentration during the process) on the key design variables, $H_2O_2$ consumption and treatment time, for a predetermined amount of wastewater decontamination. This work completes a recently published study on the influence of different inorganic ions present in wastewater in a range which clearly affects the mineralization and degradation rate of those original pollutants [18].

### 3.1. Effect of initial DOC concentration

The photo-Fenton degradation of a mixture of five commercial pesticides was studied at different initial DOC (100, 200 and 500 mg/L) to observe the effect of the initial organic content on the decontamination rate at 20 mg/L $Fe^{2+}$ and 35 °C (favorable operating conditions for this mixture [18,19]. In Table 1 and subsequent results, initial concentration of DOC included was that really measured, very often not exactly the same that intended due to the size of the pilot plant and to the excipient of the commercial pesticides. As mentioned above, $H_2O_2$ concentration was always maintained between 100 and 300 mg/L, and the DOC from each commercial pesticide was 1/5 of the total mixture. Initial DOC of the mixture and initial concentration of the active ingredients as measured by liquid chromatography is shown in Table 1.

A blank experiment with an initial DOC as high as 245 mg/L (from the commercial pesticides mixture) and addition of hydrogen peroxide (without iron) under solar radiation was also performed (see Fig. 1) to find out if there was any degradation of organics by the generation of hydroxyl radicals from the $H_2O_2$/UV process. Furthermore, as the pesticides used were commercial formulations, some unknown ingredients might also cause a photocatalytic effect. It is well known that $H_2O_2$ and UV light degrade organics to a certain extent [20,21]. In this case, the effect of $H_2O_2$/UV on these compounds was quite interesting, although so low compared to their complete degradation and mineralization rates with photo-Fenton. The results are summarized in Fig. 1. After 350 min of illumination time, the active ingredients (36, 59, 50, 79 and 40% for oxamyl, methomyl, imidacloprid, dimethoate and pyrimethanil, respectively) had been partly degraded (data not shown, only DOC was included in Fig. 1) but remained unmineralized.

It may be observed in Fig. 1 and Table 2 that, as expected, overall $H_2O_2$ consumption and illumination time required for achieving the total elimination of all the active ingredients and 65% mineralization increased with higher initial DOC, since the higher organic load requires more hydroxyl radicals, and consequently, degradation of the pesticide mixture takes longer. However, the active ingredients (considered as a whole, Σpesticides) included in the commercial formulation (oxamyl, methomyl, imidacloprid, dimethoate and pyrimethanil) were all eliminated after a certain amount of mineralization of the initial DOC (29–32%) and at the same rate (zero-order kinetics), which means that the reaction mechanism does not depend on initial organic content. The illumination time necessary for 65% mineralization was also proportional to initial DOC (125, 230 and 435 min for 107, 230 and 550 mg/L of original DOC, respectively), which reinforces the above. Similar results where obtained before with these pesticides under different experimental conditions [22] Also worthy of mention is that under the same operating conditions, less $H_2O_2$ was required for mineralizing DOC as the initial concentration increased (13.6, 8.1 and 6.3 mg $H_2O_2$ consumed/mg DOC mineralized for 107, 230 and 550 mg/L of initial DOC, respectively). As $H_2O_2$ was used more efficiently as DOC increased, this means that there was always excess $H_2O_2$ and the concentration of $OH^\bullet$ radicals (produced from Eqs. (2) and (3), a simplified photo-Fenton mechanism) was constant and governed by reaction (3). Therefore, the reaction rate measured for pesticide degradation or degradation product (DP) mineralization (Eq. (4)) did not depend on organics concentration. It is well known that excess $H_2O_2$ could be consumed by inefficient reactions (reactions not producing $OH^\bullet$ radicals), e.g., 5–7, and therefore, when the organic load in wastewater is low, fewer $OH^\bullet$ radicals are required and $H_2O_2$ is not used efficiently. This information could be useful for $H_2O_2$ dosing in a future scaled-up system for treating pesticide-polluted wastewater, as the $H_2O_2$ concentration should be kept lower as pesticide concentrations in wastewater are lower. Moreover, the process would also be more efficient from the point of view of $H_2O_2$ consumption, at higher concentrations of pollutants in wastewater.

$$Fe^{2+} + H_2O_2 \rightarrow Fe^{3+} + OH^\bullet + HO^- \quad (2)$$

$$[Fe(H_2O)]^{3+} + h\nu \rightarrow Fe^{2+} + OH^\bullet + H^+ \quad (3)$$

$$OH^\bullet + \text{pesticides} \rightarrow \text{DPs}; \quad OH^\bullet + DPs^+ \rightarrow \text{inorganics} \quad (4)$$

$$Fe^{3+} + H_2O_2 \rightarrow Fe^{2+} + HO_2^\bullet + H^+ \quad (5)$$

$$2H_2O_2 \rightarrow 2H_2O + O_2 \quad (6)$$

$$OH^\bullet + H_2O_2 \rightarrow H_2O + HO_2^\bullet \quad (7)$$

The degradation of each of the active ingredients contained in the commercial pesticide mixture (oxamyl, methomyl, imidacloprid, dimethoate and pyrimethanil) can also fit zero-order kinetics, except for dimethoate, which only fit to first order. Oxamyl, methomyl, imidacloprid and pyrimethanil each showed the same rate at the different initial concentrations as well. Table 3 shows the kinetic constants for each pesticide at different initial DOC and the corresponding linear regression coefficients.

Zero-order kinetics means that the degradation rate of each pesticide was not dependent on its concentration, but on the amount of hydroxyl radicals. Since the iron concentration was kept constant, the photoreactor was designed for complete absorption of photons and there was excess $H_2O_2$. In any case, the reaction rate was in the same range (15% standard deviation), for the four pesticides at the three concentrations tested, corroborating that the proposed

**Table 1**
Initial concentration of each active ingredient at different initial DOC of the total mixture.

| $DOC_0$ (mg/L) | Oxamyl (mg/L) | Methomyl (mg/L) | Imidacloprid (mg/L) | Dimethoate (mg/L) | Pyrimethanil (mg/L) |
|---|---|---|---|---|---|
| 107 | 42 | 10 | 8.5 | 15 | 19 |
| 230 | 79 | 22 | 21 | 32 | 47 |
| 550 | 210 | 48 | 48 | 69 | 82 |

**Table 2**
Hydrogen peroxide consumption and illumination time required for different stages of photo-Fenton degradation of the commercial pesticide mixture ($Fe^{2+}$ = 20 mg/L) at different initial DOC concentrations.

| | Complete degradation of all active ingredients | | | 65% mineralization | |
|---|---|---|---|---|---|
| $DOC_0$ (mg/L) | $t_{30W}$ (min) | $H_2O_2$ (mM) | Mineralization (DOC removal, %) | $t_{30W}$ (min) | $H_2O_2$ (mM) |
| 107 | 48 | 15 | 32 | 125 | 28 |
| 230 | 120 | 20 | 29 | 230 | 35 |
| 550 | 245 | 38 | 29 | 435 | 67 |

**Table 3**
Kinetic constants and linear regression coefficients ($R^2$) for each pesticide in the mixture treated by photo-Fenton with different initial DOC.

| $DOC_0$ (mg/L) | Oxamyl (mg/L min) | Methomyl (mg/L min) | Imidacloprid (mg/L min) | Dimethoate ($min^{-1}$) | Pyrimethanil (mg/L min) |
|---|---|---|---|---|---|
| 107 | 1.24 ($R^2$: 0.98) | 0.28 ($R^2$: 0.99) | 0.33 ($R^2$: 0.99) | 0.15 ($R^2$: 0.99) | 0.56 ($R^2$: 0.99) |
| 230 | 0.95 ($R^2$: 0.99) | 0.23 ($R^2$: 0.99) | 0.25 ($R^2$: 0.99) | 0.081 ($R^2$: 0.98) | 0.40 ($R^2$: 0.98) |
| 550 | 1.12 ($R^2$: 0.99) | 0.28 ($R^2$: 0.99) | 0.28 ($R^2$: 0.99) | 0.028 ($R^2$: 0.98) | 0.43 ($R^2$: 0.98) |

kinetic behavior is independent of compound concentration. On the other hand, for dimethoate degradation (first-order kinetics), it was found that as the initial concentration rose, the kinetic constant got lower, indicating that other pesticides and DPs affects its degradation to a greater extent than the other four pesticides.

### 3.2. Influence of temperature and its relationship with dissolved iron concentration

In previous work, the effect of temperature on photo-Fenton degradation of the commercial pesticide mixture was roughly evaluated to detect the most favorable operating temperature [18], but the reason for that obtained results remained unclear.

However, our intention here was to study the influence of temperature on the photo-Fenton degradation kinetics of the mixture of five commercial pesticides in detail and its relationship with other important operating parameters, such as the iron concentration. This was done by testing at four different temperatures (25, 35, 42 and 50 °C) with 200 mg/L of $DOC_0$ (40 mg/L from each pesticide) and 20 mg/L of $Fe^{2+}$. In these experiments, the $H_2O_2$ concentration was also kept in the range of 100–300 mg/L throughout treatment. As expected, process efficiency (more mineralization in a shorter time) increased gradually with temperature up to 42 °C, because the regeneration of ferric to ferrous ions is faster at higher temperatures. In this case, this step is rate-limiting for the overall process, and the reactions involved (Eqs. (8)–(10)) are accelerated at higher temperatures [23,24].

$$Fe^{3+} + H_2O_2 \rightarrow Fe^{2+} + HO_2^{\bullet} + H^+ \quad (8)$$

$$Fe^{3+} + R^{\bullet} \rightarrow Fe^{2+} + R^+ \quad (9)$$

$$Fe^{3+} + HO_2^{\bullet} \rightarrow Fe^{2+} + O_2 + H^+ \quad (10)$$

$$[Fe(H_2O)]^{3+} + h\nu \rightarrow Fe^{2+} + OH^{\bullet} + H^+ \quad (11)$$

However, a fast, significant loss of dissolved iron was observed at 50 °C, decreasing the degradation rate dramatically due to the reduction in the catalyst concentration, which limited the process. After 175 min of illumination time, 61% of the initial dissolved iron was lost and consequently, only 44% of mineralization was achieved, whereas at 42 °C, only 37% of iron was lost and 70% was mineralized in the same illumination time (see Fig. 2a and b). Obviously, the decreased catalyst concentration had a negative effect on the process (longer treatment time required), neutralizing the advantage of higher temperatures. This is explored further below. But it is important to remark that the design of the solar plant should take it into consideration and, for example: (i) avoid solar light concentration, (ii) avoid to operate, if possible, during so hot hours in summer or add more Fe if operation is compulsory, (iii) to recuperate heat from WW before applying photo-Fenton when the source is too hot, (iv) to keep under shadow pipelines and tanks of the solar plant or apply white paint to them. There are so different design decisions related with this statement.

To confirm that the loss of efficiency was related only to the decrease in iron during the process, another experiment was also performed at 50 °C with additional iron ($Fe^{2+}$) to compensate for the loss and maintain the concentration in steady conditions at around 20 mg/L. Table 4 and Fig. 2 summarize the results, showing mineralization, illumination time, hydrogen peroxide consumption and total iron during the experiments.

As mentioned above, as the temperature rose, less illumination time was required to reach 55% mineralization in all cases except in the experiment performed at 50 °C without addition of extra iron. Nevertheless, no significant difference was found between the experiment at 42 °C and at 50 °C in which extra iron was added to maintain the concentration at around 20 mg/L. Two main effects of iron behavior can be pointed out. Firstly, a gradual loss of iron beginning after around 100 min of illumination time until the end of the experiment was observed in all cases except at 50 °C in which around 60% of the initial iron was lost right at the beginning of the test (after only 7 min of illumination time). It is well known that the main intermediates formed in the final stage of photo-Fenton and before complete mineralization are carboxylic acids [25]. These organic acids (acetic, formic, pyruvic, maleic, oxalic acid, etc.) are known to form complexes with ferric iron [26–28] which could cause the free dissolved iron in the solution to decrease after a certain illumination time. Indeed, after around 100 min, a significant amount of pesticides were in the final stage of degradation before mineralization and 49 mg/L of formic acid and 21 mg/L of acetic acid were measured at $t_{30W}$ = 110 min. Secondly, the figure shows clearly that the higher the reaction temperature was, the higher the loss of dissolved iron, reaching a maximum at 50 °C. At 25 °C the concentration of total dissolved iron at the end of the experiment

**Table 4**
Hydrogen peroxide consumption and normalized illumination time required at different stages of photo-Fenton degradation of the commercial pesticide mixture (initial DOC = 200 mg/L) ($Fe^{2+}$ = 20 mg/L) at different temperatures.

| Temperature (°C) | Complete degradation of active ingredients | | | 55% mineralization | |
|---|---|---|---|---|---|
| | $t_{30W}$ (min) | $H_2O_2$ (mM) | % mineralization | $t_{30W}$ (min) | $H_2O_2$ (mM) |
| 25 | 117 | 18 | 33 | 172 | 22 |
| 35 | 110 | 15 | 30 | 157 | 25 |
| 42 | 100 | 17 | 31 | 120 | 24 |
| 50 | 105 | 16 | 27 | 200 | 25 |
| 50 (iron added) | 95 | 17 | 34 | 120 | 25 |

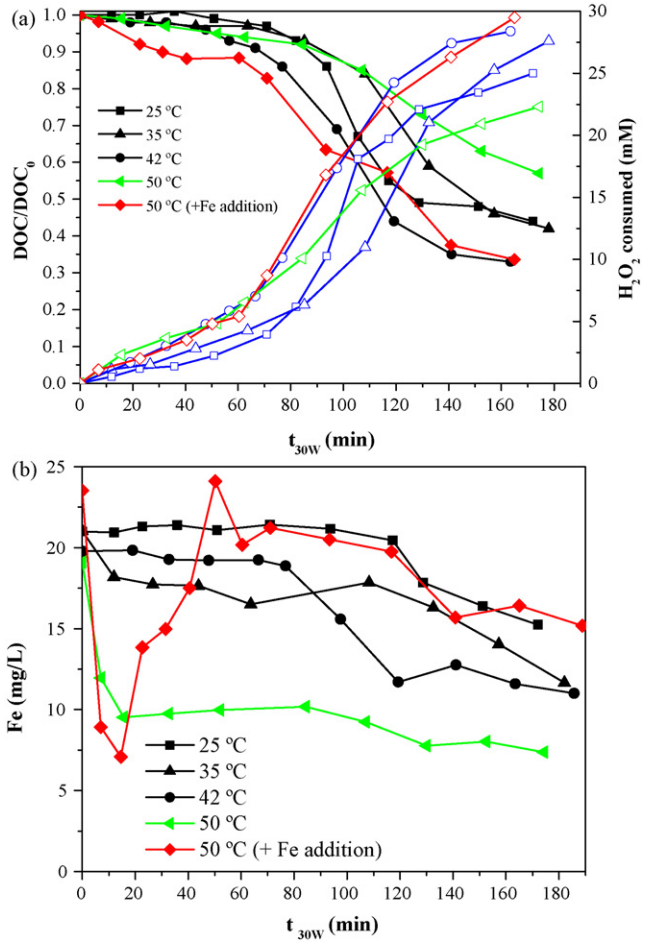


**Fig. 2.** (a) Mineralization (solid dots) of the pesticide mixture, $H_2O_2$ consumed (open dots) and (b) iron concentration during photo-Fenton experiments at the different temperatures tested.

was still 15 mg/L while the loss at 35/42 °C led to a final concentration of around 12 mg/L. The lowest concentration was at 50 °C with a final concentration of 7 mg/L. Efficiency was noticeably lower at 50 °C due to the significant decrease in the catalyst concentration. This loss of iron at 50 °C is associated mainly with the precipitation of part of the dissolved iron in the solution as ferric hydroxides according to the mechanism described in reactions (12)–(15) [29]

$$Fe^{3+} + H_2O \leftrightarrow FeOH^{2+} + H^+ \quad (12)$$

$$FeOH^{2+} + H_2O \leftrightarrow Fe(OH)^{2+} + H^+ \quad (13)$$

$$Fe(OH)^{2+} + H_2O \leftrightarrow Fe(OH)_3 + H^+ \quad (14)$$

$$Fe(OH)_3 \leftrightarrow Fe(OH)_3(solid) \quad (15)$$

Ferric hydroxides precipitate at a lower pH than ferrous iron. In the absence of further complexing substances, because of the low solubility product of ferric iron hydroxide ($K_S(Fe(OH)_3) \approx 10^{-37}$), precipitation starts at pH 2.5–3.5 depending on the iron concentration, while the ferrous hydroxides precipitate mainly at a pH up to 6 [30] Precipitation, which also depends on temperature, according to Sapieszko [31], is higher and faster as temperature increases from 25 to 80 °C. Other authors have previously observed the precipitation of total dissolved iron during the photo-Fenton treatment of dark-black coffee effluent, although in this case, no temperature effect on increased iron precipitation was observed, as the experiments were conducted at room temperature [32] The first step in precipitation is the formation of dimmers and oligomers. As polymerization continues, the compound grows, while losing water until the insoluble iron hydroxide (e.g. goethite or hematite) precipitates. The resulting amorphous ferric oxyhydroxides still contain a lot of water, are red-brown, and absorb over the whole UV/vis spectral range. As ferric compounds are strongly cationic, coprecipitation with other ions and organic substances can take their place, which is why iron is used as a coagulant in other processes. Although in photo-Fenton, the majority of the dissolved iron is ferric, some photo-regenerated ferrous iron could also be precipitated with ferric iron-oxyhydroxides [14]. On the other hand, no significant difference from temperature variation was detected in hydrogen peroxide consumption, which remained the same for a given mineralization (see Fig. 2). This means that temperature only affected iron precipitation, and consequently degradation rate, while hydrogen peroxide continued to be used efficiently in all the experiments, because only iron precipitation was responsible for the lower degradation rate.

Another point to consider is that although the strong iron precipitation at 50 °C led to a decrease in overall photo-Fenton efficiency (longer illumination time required for mineralization), the differences in degradation of the five active ingredients contained in the commercial pesticides were not so significant. The illumination time required for the total elimination of the active compounds and the $H_2O_2$ consumed was comparable at all temperatures (see Table 4). Moreover, the degradation kinetics of the active ingredients was similar in all cases. The kinetics constants calculated for each active ingredient at the four temperatures are summarized in Table 5. The degradation rate of all the individual active ingredients was observed to increase slightly with temperature up to 42 °C, and was similar at 42 and 50 °C, independent of iron precipitation. It may be concluded that acceleration of reactions (2)–(4) at higher temperatures can compensate for the loss of iron in the degradation of the parent compounds, but as degradation proceeds and more stable DPs are formed (for example, carboxylic acids), the lack of iron becomes detrimental to overall mineralization.

### 3.3. Blank tests

In view of the above results and the important role of iron in photo-Fenton, some additional studies were performed for a more in-depth study of the behavior of iron and $H_2O_2$ consumption at different temperatures. The main purpose of these tests was to

**Table 5**
Kinetic constants and linear regression coefficients ($R^2$) for each pesticide in the mixture treated by photo-Fenton at different temperatures ($DOC_0$: 200 mg/L; $Fe_0^{2+}$: 20 mg/L).

| Temperature (°C) | Oxamyl (mg/L min) | Methomyl (mg/L min) | Imidacloprid (mg/L min) | Dimethoate ($min^{-1}$) | Pyrimethanil (mg/L min) |
|---|---|---|---|---|---|
| 25 | 0.6 ($R^2$: 0.97) | 0.19 ($R^2$: 0.98) | 0.21 ($R^2$: 0.98) | 0.029 ($R^2$: 0.97) | 0.45 ($R^2$: 0.99) |
| 35 | 0.67 ($R^2$: 0.99) | 0.23 ($R^2$: 0.99) | 0.21 ($R^2$: 0.98) | 0.045 ($R^2$: 0.99) | 0.40 ($R^2$: 0.98) |
| 42 | 1.17 ($R^2$: 0.99) | 0.34 ($R^2$: 0.98) | 0.32 ($R^2$: 0.99) | 0.048 ($R^2$: 0.98) | 0.67 ($R^2$: 0.98) |
| 50 | 0.97 ($R^2$: 0.98) | 0.34 ($R^2$: 0.99) | 0.29 ($R^2$: 0.99) | 0.066 ($R^2$: 0.98) | 0.60 ($R^2$: 0.99) |

**Table 6**
$H_2O_2$ consumption and final iron concentration after 180 min of reaction ($Fe^{2+}_0$: 20 mg/L, 300 mg/L $H_2O_2$) in absence (blank) and presence of the pesticide mixture ($DOC_0$: 200 mg/L) at four different temperatures in the dark.

| Temperature | 25 °C | | 35 °C | | 42 °C | | 50 °C | |
|---|---|---|---|---|---|---|---|---|
| | Blank | Pest | Blank | Pest | Blank | Pest | Blank | Pest |
| $H_2O_2$ cons. (mM) | 4 | 0.5 | 5.7 | 1.6 | 5.9 | 2.5 | 6.2 | 4 |
| Final Fe conc. (mg/L) | 8 | 19 | 6 | 15 | 6.5 | 13 | 5.5 | 10 |

improve our understanding of the ongoing reactions and validate the hypotheses above. Some blank tests were therefore carried out under the same operating conditions as the previous photo-Fenton tests. The parameters monitored were $H_2O_2$ consumption and the dissolved iron concentration. The results are summarized in Table 6 and Fig. 3.

Several significant trends may be observed in these results, in agreement with the results of photo-Fenton tests but clarifying the key parameters involved in the processes. There is an explicit difference between the results of the experiments with and without pesticides in both parameters (iron loss and $H_2O_2$ consumption) in the dark and under irradiation, which are significantly higher in absence of the organic compounds. The larger amount of dissolved iron and its slower precipitation in presence of the pesticides (Fig. 3, A1) can be explained by complexation processes, which stabilized the iron, thereby partly averting the precipitation of iron hydroxide [28] As mentioned, ferric iron is crucial to precipitation at a pH below 3. Whereas, the ferric iron can be regenerated to ferrous iron in the photo-Fenton reaction under UV-radiation, this regeneration step is known to be very slow in the dark [14] Therefore, the concentration of ferric iron was always high and in the absence of organic molecules (Fig. 3, A2 and A3), all the ferric iron can precipitate

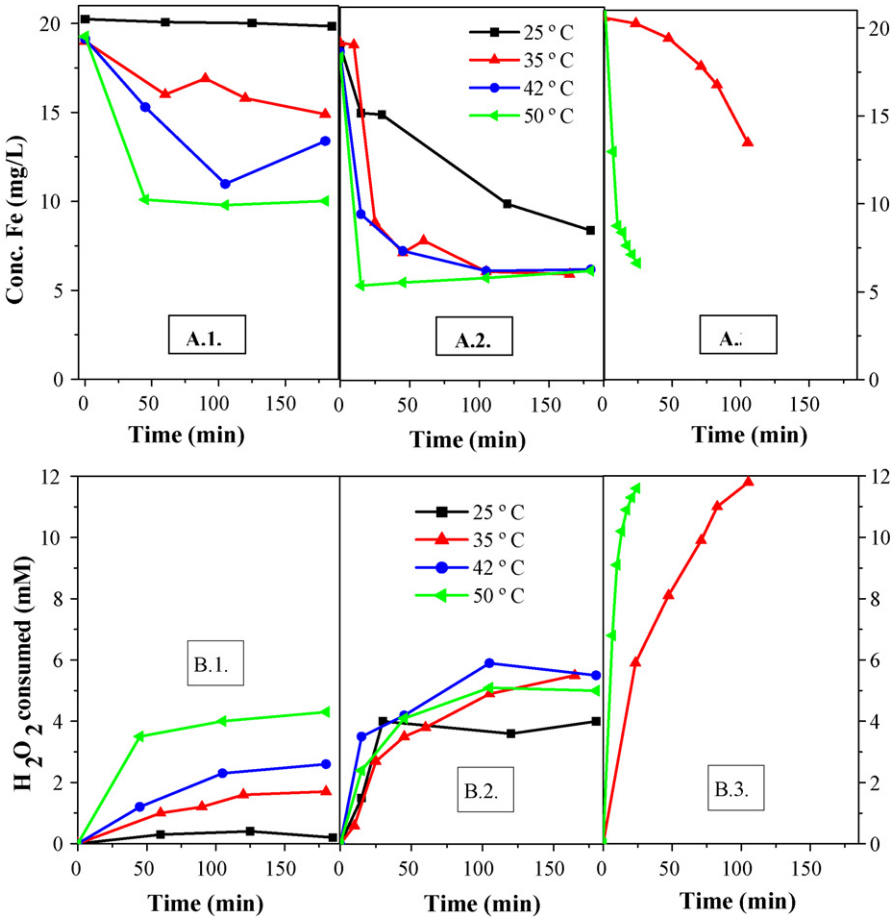


**Fig. 3.** Iron concentration and $H_2O_2$ consumption ($Fe^{2+}_0$: 20 mg/L, 100–300 mg/L $H_2O_2$) in the dark and with pesticides (A.1, B.1), in the dark and in absence of pesticides (A.2, B.2) and under irradiation and absence of pesticides (A.3, B.3) at different operating temperatures.

more easily as ferric hydroxides. With regard to $H_2O_2$ consumption, in the presence of organics (Fig. 3, B1), the peroxyl radical can regenerate hydrogen peroxide, reacting with dissolved oxygen according to reactions (16)–(18), and reducing $H_2O_2$ consumption [33] On the contrary, in the absence of organics (Fig. 3, B2), the hydroxyl radicals generated can react easily with the hydrogen peroxide (reaction (7)) and the $H_2O_2$ self-decomposition reaction is also easier (reaction (6)). This explains the increase in the overall $H_2O_2$ consumption when there are no pesticides present. It may also be observed that, as expected, $H_2O_2$ consumption was noticeably higher in the presence of irradiation (Fig. 3, B3). Since, as also mentioned above, the regeneration of ferrous iron from ferric iron is very slow in the absence of irradiation, the reaction between ferrous ion and hydrogen peroxide is limited and consequently, less $H_2O_2$ is consumed.

$$R + O_2 \rightarrow RO_2^{\bullet} \quad (16)$$

$$RO_2^{\bullet} + H_2O \rightarrow ROH + H_2O^{\bullet} \quad (17)$$

$$HO_2^{\bullet} + H_2O_2 + O_2 \quad (18)$$

In the presence of organic molecules, dissolved iron decreased more as the temperature rose. These results were consistent with the previous photo-Fenton experiments with iron precipitation. Iron loss was higher as the temperature rose (reaching a maximum at 50 °C), and the final dissolved iron concentrations were similar in the blank and the photo-Fenton tests at all four temperatures. However, in the dark and with pesticides, a clear dependence between temperature and $H_2O_2$ consumption was observed. As the concentration of ferric ions in the blank experiments is always higher than in the photo-Fenton reaction, $H_2O_2$ can be consumed in undesirable reactions (reaction (5)) accelerated by the increase in temperature.

## 4. Conclusions

Solar photo-Fenton scale-up needs to take into account the main operating parameters, such as temperature, $H_2O_2$ consumption and catalyst ($Fe^{2+}$ or $Fe^{3+}$) dose, which strongly depend on the organic load and composition of the wastewater to be treated. From the results of the study of these parameters on a synthetic industrial wastewater, it can be concluded that solar plants should be designed for operating at temperatures below 45 °C to avoid significant loss of iron, as the loss of efficiency at higher temperatures was related to the decrease in iron concentration due to precipitation during the process. This effect can be partly compensated by iron complexation by certain wastewater components. On the other hand, $H_2O_2$ should be carefully dosed during the photo-Fenton treatment to avoid its continued excess and inefficient use. This is even more crucial when the target wastewater does not have a very high organic load, as careful dosing of $H_2O_2$ is more important the lower the organic load of the wastewater is. These statements reinforce the need for optimizing the $H_2O_2$ dose and iron concentration for photo-Fenton wastewater treatment case-by-case.

## Acknowledgments

The authors wish to thank the Spanish Ministry of Education and Science for its financial assistance under the “Fotobiox” Project (Ref. CTQ2006-14743-C03-01). They also wish to thank Mrs. Deborah Fuldauer for correcting the English. Luigi Rizzo wishes to thank the University of Salerno (Italy) and the Province of Salerno for the research grant which allowed him to work in the above mentioned project at the Plataforma Solar de Almeria.

## References

[1] S. Suárez, M. Carballa, F. Omil, J.M. Lema, Rev. Environ. Sci. Biotechnol. 7 (2008) 125–138.
[2] Directive 2008/105/EC of the European parliament and of the council of December 16, 2008.
[3] M. Klavarioti, D. Mantzavinos, D. Kassinos, Environ. Int. 35 (2009) 402–417.
[4] C. Comninellis, A. Kapalka, S. Malato, S.A. Parsons, I. Poulios, D. Mantzavinos, J. Chem. Technol. Biotechnol. 83 (2008) 769–776.
[5] J.A. Giroto, A.C. Teixeira, C.A. Nascimiento, R. Guardani, Chem. Eng. Process. 47 (2008) 2361–2369.
[6] P.M. Álvarez, F.J. Beltrán, F.J. Masa, J.P. Pocostales, Appl. Catal. B 92 (2009) 393–400.
[7] F. Han, V. Kambala, M. Srinivasan, Appl. Catal. A 359 (2009) 25–40.
[8] P.R. Gogate, A.B. Pandit, Adv. Environ. Res. 8 (2004) 553–597.
[9] F.I. Hai, K. Yamamoto, K. Fukushi, Crit. Rev. Environ. Sci. Technol. 37 (2007) 315–377.
[10] I. Muñoz, J. Rieradevall, J. Torrades, F. Peral, X. Domènech, Chemosphere 62 (2006) 9–16.
[11] M.J. Farré, J. García-Montaño, N. Ruiz, I. Múñoz, X. Domènech, J. Peral, Environ. Technol. 28 (2007) 819–830.
[12] I. Muñoz, S. Malato, A. Rodríguez, X. Doménech, J. Adv. Oxid. Technol. 11 (2008) 270–275.
[13] S. Malato, P. Fernández-Ibáñez, M.I. Maldonado, J. Blanco, W. Gernjak, Catal. Today 147 (2009) 1–59.
[14] J. Pignatello, E. Oliveros, A. MacKay, Crit. Rev. Environ. Sci. Technol. 36 (2006) 1–84.
[15] R.F.P. Nogueira, M.C. Oliveira, W.C. Paterlini, Talanta 66 (2005) 86–91.
[16] M. Lapertot, C. Pulgarín, P. Fernández-Ibáñez, M.I. Maldonado, L. Pérez-Estrada, I. Oller, W. Gernjak, S. Malato, Water Res. 40 (2006) 1086–1094.
[17] S. Malato, J. Blanco, A. Vidal, D. Alarcón, M.I. Maldonado, J. Cáceres, W. Gernjak, Sol. Energy 75 (2003) 329–336.
[18] A. Zapata, I. Oller, E. Bizani, J.A. Sánchez-Pérez, M.I. Maldonado, S. Malato, Catal. Today 144 (2009) 94–99.
[19] A. Zapata, T. Velegraki, J.A. Sánchez-Pérez, D. Mantzavinos, M.I. Maldonado, S. Malato, Appl. Catal. B 88 (2009) 448–454.
[20] E. Kowalska, M. Janczarek, J. Hupka, M. Grynkiewicz, Water Sci. Technol. 49 (2004) 261–266.
[21] J.C. Kruithof, P.C. Kamp, B.J. Martijn, Ozone Sci. Eng. 29 (2007) 273–280.
[22] M.M. Ballesteros, J.A. Sánchez Pérez, J.L. García-Sánchez, J.L. Casas, S. Malato, Water Res. 43 (2009) 3838–3848.
[23] G. Sagawe, A. Lehnard, M. Lübber, D. Bahnemann, Helv. Chem. Acta 84 (2001) 3742–3759.
[24] C. Lee, J. Yoon, Chemosphere 56 (2004) 923–934.
[25] H.D. Burrows, L.M. Canle, J.A. Santaballa, S. Steenken, J. Photochem. Photobiol. B 67 (2002) 71–108.
[26] B. Faust, J. Hoigné, Atmos. Environ. 24 (1990) 79–89.
[27] B. Sulzberger, H. Laubscher, Mar. Chem. 50 (1995) 103–115.
[28] M. Fujii, H. Ito, A.L. Rose, T.D. Waite, T. Omura, Geochim. Cosmochim. Acta 72 (2008) 6079–6089.
[29] T. Grundl, J. Delwiche, J. Contam. Hydrol. 14 (1993) 71–97.
[30] N.C. Datta, J. Sci. Ind. Res. 40 (1981) 571–583.
[31] R.S. Sapieszko, R.C. Patel, E. Matijevic, J. Phys. Chem. 81 (1977) 1061–1068.
[32] M. Tokumura, A. Ohta, H.T. Znad, Y. Kawase, Water Res. 40 (2006) 3775–3784.
[33] C. Von Sonntag, P. Dowideit, X. Fang, R. Mertens, X. Pan, M.N. Schuchmann, H.P. Schuchmann, Water Sci. Technol. 35 (1997) 9–15.